Identification of CLN6 as a molecular entity of endoplasmic reticulum-driven anti-aggregate activity

Arisa Yamashita, Yuri Hiraki, Tetsuo Yamazaki*

Department of Molecular Cell Biology and Medicine, Graduate School of Biomedical Sciences, Tokushima University, 1-78-1, Sho-machi, Tokushima 770-8505, Japan

* Corresponding author. TEL: +81 88 633 7886 FAX: +81 88 633 9550.
E-mail address: tyamazak@tokushima-u.ac.jp (T. Yamazaki).

Abstract

αB-crystallin (αBC) is a small heat shock protein. Mutations in the αBC gene are linked to α-crystallinopathy, a hereditary myopathy histologically characterized by intracellular accumulation of protein aggregates. The disease-causing R120G αBC mutant, harboring an arginine-to-glycine replacement at position 120, is an aggregate-prone protein. We previously showed that the R120G mutant's aggregation in HeLa cells was prevented by enforced expression of αBC on the endoplasmic reticulum (ER). To elucidate the molecular nature of the preventive effect on the R120G mutant, we isolated proteins binding to ER-anchored αBC (TMαBC). The ER transmembrane CLN6 protein was identified as a TMαBC's binder. CLN6 knockdown in HeLa cells attenuated TMαBC's anti-aggregate activity against the R120G mutant. Conversely, CLN6 overexpression enhanced the activity, indicating that CLN6 operates as a downstream effector of TMαBC. CLN6 physically interacted with the R120G mutant, and repressed its aggregation in HeLa cells even when TMαBC was not co-expressed. Furthermore, CLN6's antagonizing effect on the R120G mutant was compromised upon treatment with a lysosomal inhibitor, suggesting CLN6 requires the intact autophagy-

lysosome system to prevent the R120G mutant from aggregating. We hence conclude that CLN6 is not only a molecular entity of the anti-aggregate activity conferred by the ER manipulation using TMαBC, but also serves as a potential target of therapeutic interventions.

Keywords

αB-crystallin, aggregate, CLN6, endoplasmic reticulum, neuronal ceroid lipofuscinosis

1. Introduction

αBC is a member of the small heat shock protein family. Mutations in the αBC gene are linked to α-crystallinopathy, an autosomal dominantly inherited myopathy [1]. The pathogenesis of this disease is poorly understood and there is no curative therapy available. Histologically, α-crystallinopathy is characterized by accumulation of aberrant protein aggregates in cardiomyocytes and skeletal myocytes. Formation of protein aggregates is closely associated with a wide array of degenerative neuromuscular disorders, including amyotrophic lateral sclerosis, Alzheimer's disease and α-crystallinopathy [2–5]. Molecular mechanisms underlying aggregate accumulation have thus been investigated and therapeutic interventions with which to antagonize aggregate-prone proteins have been required to be established. The disease-causing R120G αBC mutant is one of those proteins with aggregation propensities, and aggregates when transfected into non-muscle cell lines [6]. We previously showed that aggregation of the R120G mutant in HeLa cells was prevented by co-expressed TMαBC, and hypothesized that some proteins situated on the ER were manipulated via interactions with TMαBC, thereby exerting their anti-aggregate activity toward the R120G mutant [7]. To reveal the molecular basis of this ER-based antagonistic action on the aggregate-prone mutant, we purified TMαBC-binding proteins. Here we identified CLN6, an ER transmembrane protein linked to neuronal

ceroid lipofuscinosis [8–10], as an effector molecule operating downstream of TMαBC. Based on our results, we propose that CLN6 has anti-aggregate activity and would be a promising target in developing therapeutic strategies for protein aggregation diseases.

2. Materials and methods

2.1. Expression vectors and small interfering RNAs

The construction of the following expression vectors was described previously [11,12]: pEGFP-N1-R120G αBC mutant (R120G-EGFP), pcDNA4/myc-αBC (WTαBC), and pcDNA4/myc-TMαBC (TMαBC). The DNA fragment encoding human CLN6 was PCR-generated using the following primers: 5'-GGCAAGCTTCACCATGGAGGCGACGCGGAGGCGGC-3' and 5'-GCCGTCGACGAATTCCAGTGCCGACTGCTGACGTG-3'. The template was cDNA synthesized with the GoScript Reverse Transcription System (Promega) employing RNA isolated from HeLa cells. The PCR product was digested with HindIII/SalI, and then cloned in frame into the HindIII/SalI-digested pEGFP-N1vector (TAKARA Bio). The resulting pEGFP-N1-CLN6 (CLN6-EGFP) expression construct was digested with HindIII/EcoRI to yield the DNA fragment corresponding to full-length CLN6. This fragment was then cloned in frame into the HindIII/EcoRI-digested pcDNA4/myc-His vector (Invitrogen), generating pcDNA4/myc-CLN6 (CLN6). All the constructs were subjected to DNA sequencing. To knock down CLN6, two different siRNA duplexes (Sigma-Aldrich) as below were individually transfected into HeLa cells: siCLN6a (5′-CUCUCGAGUGGUUUCCACUTT-3′ and 5′-AGUGGAAACCACUCGAGAGTT-3′) and siCLN6b (5′-CCCUCUUGCUUGUGGCGCUTT-3′ and 5′-AGCGCCACAAGCAAGAGGGTT-3′). The siRNA duplex against ATG5 (siATG5) was described previously [12].

2.2. Cell culture and transfection

HeLa cells were maintained in αMEM (nacalai tesque, Japan) supplemented with 10% fetal bovine serum at 37 °C in a humidified cell culture incubator with 5% CO_2. For transfection, the cells were seeded at 1.5 x 10^4 cells per well onto 24-well plates or 35-mm glass bottom dishes 20 h prior to transfection. The cells in each well were transfected with single (0.4 μg) or two different (0.2 μg each) expression constructs mixed with 1.2 μl of PEI "Max" (Polysciences), or 0.34 μg of siRNA mixed with 2 μl of the X-tremeGENE siRNA transfection reagent (Roche).

2.3. Reverse transcription polymerase chain reaction analysis

Reverse transcription polymerase chain reaction (RT-PCR) was performed as described previously [13]. Primers used were as follows: 5′-GCATTGCTGACAGGATGCAG-3′ and 5′-CCTGCTTGCTGATCCACATC-3′ for β-actin, 5′-GCATGGCTCTGTGAGCGCTGATGAGGCTG-3′ and 5′-GCAGAATTCGAGTCACCCACCAGGTGGATGCTG-3′ for CLN6.

2.4. Antibodies

Antibodies used are as follows: Actin (diluted 1:200, Santa Cruz Biotech, C-2, sc-8432), ATG5 (diluted 1:1000, Cell Signaling, #2630), CLN6 (diluted 1:200, abcam, ab82786), LC3-I/II (diluted 1:500, Cell Signaling, #12741), c-Myc (diluted 1:200, Santa Cruz Biotech, 9E10, sc-40), GFP (diluted 1:1000, MBL, #598), and horse radish peroxidase (HRP)-conjugated antibodies (diluted 1:3000, rabbit anti-mouse IgG and goat anti-rabbit IgG, both from DAKO).

2.5. Immunoblot analysis

At 16 h post-transfection, HeLa cells were solubilized in RIPA lysis buffer (100 mM Tris (pH 7.5), 150 mM NaCl, 2 mM EDTA, 1% TrironX-100, 1% DOC and 0.1% SDS plus protease inhibitor cocktail) and incubated on ice for 30 min, then centrifuged at

14,800 rpm for 10 minutes. Soluble fraction was collected, mixed with 2X Laemmli buffer, boiled, resolved by SDS–PAGE, and electrotransferred onto polyvinylidene difluoride membranes. The membranes were then incubated with primary and secondary antibodies described in 2.4 Antibodies. HRP on the membrane was detected using the *ImmunoStar* luminescence solution (Wako Pure Chemical Industries, Japan) according to the manufacturer's instruction.

2.6. Immunoprecipitation assay

At 16 h post-transfection, HeLa cells were solubilized in lysis buffer (50 mM Tris (pH 8.0) and 150 mM NaCl with 1% NP-40 plus protease inhibitor cocktail). The lysates were incubated with antibodies against myc or GFP overnight at 4 °C, subjected to incubation with protein A-Sepharose (GE Healthcare Life Sciences) for another hour. Subsequently, the immunoprecipitates were resolved by SDS–PAGE and electrotransferred onto polyvinylidene difluoride membranes for immunoblotting with specific antibodies.

2.7. Mass spectrometric analysis

Myc immunoprecipitates derived from 1.5 x 10^4 transfected HeLa cells were separated by SDS-PAGE. The gel was stained using Pierce® Silver Stain for Mass Spectrometry (Thermo Fisher Scientific) according to the manufacture's protocol. The bands selected as potential binding partners of TMαBC were excised and in-gel digested with trypsin according to a previously published method [14]. The digested peptides were subjected to liquid chromatography-mass spectrometry/mass spectrometry (LC-MS/MS) analysis. Nano liquid chromatography of these peptides and the mass spectrometric analysis were performed with the UltiMate 3000 RSLCnano system (Thermo Fisher Scientific) and an Orbitrap Elite mass spectrometer (Thermo

Fisher Scientific), respectively. The data was analyzed with Mascot (Matrix Science) MS/MS Ion Search to assign the obtained peptides to the NCBI database.

2.8. Measurement of aggregate positivity

At 16 h post-transfection, live HeLa cells expressing EGFP-tagged R120G αBC mutant were subjected to confocal microscopic analysis. EGFP images were acquired using a Zeiss LSM-700 confocal microscope with 20x/0.75 NA dry objective, and analyzed with the ZEN Lite software (Carl Zeiss Inc.). Based on the images, the percentage of cells with aggregates in EGFP-positive cells was calculated. At least 800 cells were analyzed for each condition in every assay.

2.9. Statistical analysis

All data is expressed as means ± S.E.M. The data was accumulated under each condition from at least seven independent experiments. For non-parametric all-pairs multiple comparisons, Steel–Dwass test was used.

3. Results

3.1 CLN6 was identified as a binding partner of TMαBC

TMαBC prevented the R120G mutant from aggregating, while wild-type αBC (WTαBC), which is scattered throughout the cytoplasm, did not. The finding prompted us to reason that proteins possessing anti-aggregate activity are situated on the ER, cooperating with TMαBC. To elucidate the molecular nature of TMαBC's preventive effect on aggregate formation, we purified and mass spectrometrically analyzed proteins that specifically bound to TMαBC (Suppl. Fig. 1). One of the identified proteins was the ER-resident transmembrane CLN6 protein, variants of which are linked to neuronal ceroid lipofuscinosis, classified as a lysosomal storage disease. To validate CLN6's interaction with TMαBC, HeLa cells were co-transfected with an

EGFP-tagged version of CLN6 plus either myc-tagged TMαBC or WTαBC, subjected to co-immunoprecipitation assays. CLN6 co-immunoprecipitated with TMαBC, but not with WTαBC (Fig. 1), further supporting specific physical interactions between CLN6 and TMαBC.

3.2 CLN6 was a downstream effector of TMαBC

The demonstrated physical interactions led us to postulate that CLN6 operates downstream of TMαBC. To explore this possibility, we investigated if CLN6 knockdown impairs TMαBC's anti-aggregate activity toward the R120G mutant. Two different siRNA duplexes (siCLN6a and siCLN6b) were separately used to silence the CLN6 gene, and depletion of CLN6 in HeLa cells was verified at both transcript and protein levels (Fig. 2A, B). The siRNA-transfected cells were subsequently co-transfected with the R120G mutant plus TMαBC, subjected to microscopic analysis (Fig. 2C). Aggregate positivity in CLN6-depleted cells was ~25% higher than that in CLN6-sufficient counterparts (Fig. 2D), indicating that TMαBC's preventive effect on the R120G mutant is mediated, at least in part, by CLN6.

3.3 CLN6 prevented aggregate formation without the guidance of TMαBC

We further explored whether CLN6 exerts anti-aggregate activity against the R120G mutant even without cooperation of TMαBC. When co-transfected with the R120G mutant into HeLa cells, CLN6 mitigated the R120G mutant-mediated aggregate formation to a similar extent as TMαBC (Fig. 3A, B). In contrast, CLN6 knockdown in HeLa cells elevated aggregate positivity by approximately 25%, compared with the control knockdown (Fig. 3C). Given that myc-tagged CLN6 co-immunoprecipitated with the R120G mutant tagged with EGFP (Fig. 3D), we concluded that endogenous CLN6 serves to prevent the mutant from aggregating in a TMαBC-independent manner

as well, which would be underpinned by physical interactions between CLN6 and the mutant.

3.4 CLN6 required the autophagy-lysosome system to counter the R120G mutant

Integrity of the autophagy-lysosome system is essential to prevent aggregate accumulation [15,16]. We thus investigated if inhibitors of the proteolytic system affect CLN6's anti-aggregate activity toward the R120G mutant. Bafilomycin A1, a lysosomal inhibitor, elevated the aggregate positivity in a dose-dependent manner, whereas the MG132 proteasome inhibitor did not significantly affect the aggregate formation (Fig. 4A), indicating CLN6 antagonizes the R120G mutant by utilizing the autophagy-lysosome pathway. We further assessed the autophagy dependency of CLN6 using siRNA against ATG5, a protein involved in earlier steps of autophagy [17]. ATG5-depleted HeLa cells and their counterparts displayed comparable aggregate positivity following co-transfection with CLN6 plus the R120G mutant (Fig. 4B, C). Like TMαBC, CLN6 appeared to employ an ATG5-independent autophagic pathway to counter the mutant when an ATG5-dependent pathway is not available. Of note, neither overexpressed CLN6 nor TMαBC elevated LC3-II protein levels, one of the indicators of autophagic flux [18] (Fig. 4D). Rather than upregulating the autophagy-lysosome system, CLN6 was suggested to protect the system from detrimental effects of aggregate-prone proteins.

4. Discussion

We previously demonstrated that overexpression of TMαBC, but not of WTαBC, prevents aggregation of the disease-causing R120G αBC mutant, proposing that some proteins situated on the ER are manipulated by TMαBC and help repress aggregate formation. Here we identified CLN6 as a binding partner and downstream effector of TMαBC. Although evenly distributed across the cytoplasm, WTαBC did not bind to

CLN6, implying that there are as-yet-unidentified obstacles surrounding the ER membrane that hamper WTαBC's access to CLN6. When tethered to the ER membrane, αBC is most likely to override such obstacles and readily reach CLN6. Considering that TMαBC bound to the R120G mutant, the mutant would be brought into the proximity CLN6 primed by TMαBC to exhibit its anti-aggregate activity. Alternatively, TMαBC could derepress rather than stimulate CLN6. There might be proteins negatively regulating CLN6 through physical interactions. TMαBC would bind to and dissociate those potentially inhibitory proteins from CLN6, unleashing the anti-aggregate activity of CLN6. This scenario could explain why overexpressed CLN6 prevented aggregation of the R120G mutant without assistance from TMαBC. In this case, CLN6 would outnumber inhibitory proteins. As a result, a considerable amount of CLN6 can escape the restraint and readily act on the R120G mutant. Either way, formation of a multi-protein complex including CLN6 and the R120G mutant as its component is most likely to be the driving force behind the observed anti-aggregate activity.

Integrity of the autophagy-lysosome system was required for CLN6 to antagonize the R120G mutant. CLN6, however, appeared not to upregulate autophagy, given that overexpression of CLN6 had no appreciable impacts on LC3-II protein levels. We hence reasoned that CLN6, rather than enhancing autophagy, just nullify the R120G mutant's aggregate-prone properties. The mutant might be structurally constrained by CLN6, remaining as an aggregate precursor not detrimental to the autophagy-lysosome machinery. ATG5-dependent and/or -independent autophagic pathways would likely be kept functional and engaged in clearance of the resulting aggregate precursors.

Mutations in the CLN6 gene are linked to variant late-infantile neuronal ceroid lipofuscinosis (vLINCL) [10,19], classified as a lysosomal storage disorder. Numerous aggregates positive for the autophagy-related protein p62 have been found in brains of the *nclf* mouse model of vLINCL [20], where the CLN6 protein is prematurely

truncated. This is consistent with our findings that CLN6 knockdown augmented the R120G mutant-mediated aggregate formation. CLN6 is most likely to antagonize aggregate-prone proteins in an individual mouse as well. In this regard, quantitatively upregulating CLN6 would thus be therapeutically effective for vLINCL, provided that accumulation of the p62-aggregate is central to the pathogenesis of vLINCL.

We previously demonstrated that manipulation of the microenvironment surrounding the ER membrane would likely be beneficial for developing therapeutic strategies against α-crystallinopathy, characterized by intracellular accumulation of protein aggregates. Here, we not only identified CLN6 as a target of the ER manipulation, but also have given novel etiological insights into how defects in the ER-resident CLN6 protein are associated with alterations in an anatomically distinct compartment of the lysosome.

Acknowledgements

This work was supported by JSPS KAKENHI Grant Numbers JP15K08404 and JP16J0978, and by A Strategic Project for Innovative Research "iPUT" from Tokushima University.

References

[1] A. Sanbe, Molecular mechanisms of α-crystallinopathy and its therapeutic strategy., Biol. Pharm. Bull. 34 (2011) 1653–1658.

[2] D.C. Rubinsztein, The roles of intracellular protein-degradation pathways in neurodegeneration, Nature. 443 (2006) 780–786.

[3] P. Castets, S. Frank, M. Sinnreich, M.A. Rüegg, "Get the Balance Right": Pathological Significance of Autophagy Perturbation in Neuromuscular Disorders, J. Neuromuscul. Dis. 3 (2016) 127–155.

[4] C.J. Roberts, Therapeutic protein aggregation: mechanisms, design, and control, Trends Biotechnol. 32 (2014) 372–380.

[5] A. Ciechanover, Y.T. Kwon, Degradation of misfolded proteins in neurodegenerative diseases: therapeutic targets and strategies, Exp. Mol. Med. 47 (2015) e147.

[6] P. Vicart, A. Caron, P. Guicheney, Z. Li, M.-C. Prévost, A. Faure, D. Chateau, F. Chapon, F. Tomé, J.-M. Dupret, D. Paulin, M. Fardeau, A missense mutation in the αB-crystallin chaperone gene causes a desmin-related myopathy, Nat. Genet. 20 (1998) 92–95.

[7] S. Yamamoto, T. Yamazaki, S. Komazaki, T. Yamashita, M. Osaki, M. Matsubayashi, H. Kidoya, N. Takakura, D. Yamazaki, S. Kakizawa, Contribution of calumin to embryogenesis through participation in the endoplasmic reticulum-associated degradation activity., Dev. Biol. 393 (2014) 33–43.

[8] S.E. Mole, G. Michaux, S. Codlin, R.B. Wheeler, J.D. Sharp, D.F. Cutler, CLN6, which is associated with a lysosomal storage disease, is an endoplasmic reticulum protein, Exp. Cell Res. 298 (2004) 399–406.

[9] C. Heine, B. Koch, S. Storch, A. Kohlschütter, D.N. Palmer, T. Braulke, Defective endoplasmic reticulum-resident membrane protein CLN6 affects lysosomal degradation of endocytosed arylsulfatase A, J. Biol. Chem. 279 (2004) 22347–22352.

[10] K. Kollmann, K. Uusi-Rauva, E. Scifo, J. Tyynelä, A. Jalanko, T. Braulke, Cell biology and function of neuronal ceroid lipofuscinosis-related proteins, Biochim. Biophys. Acta - Mol. Basis Dis. 1832 (2013) 1866–1881.

[11] A. Yamashita, T. Taniwaki, Y. Kaikoi, T. Yamazaki, Protective role of the endoplasmic reticulum protein mitsugumin23 against ultraviolet C-induced cell death, FEBS Lett. 587 (2013) 1299–1303.

[12] S. Yamamoto, A. Yamashita, N. Arakaki, H. Nemoto, T. Yamazaki, Prevention of aberrant protein aggregation by anchoring the molecular chaperone αB-crystallin to the endoplasmic reticulum., Biochem. Biophys. Res. Commun. 455 (2014) 241–245.

[13] T. Yamazaki, T. Kurosaki, Contribution of BCAP to maintenance of mature B cells through c-Rel, Nat. Immunol. 4 (2003) 780–786.

[14] A. Shevchenko, M. Wilm, O. Vorm, M. Mann, Mass spectrometric sequencing of proteins silver-stained polyacrylamide gels., Anal. Chem. 68 (1996) 850–858.

[15] T. Hara, K. Nakamura, M. Matsui, A. Yamamoto, Y. Nakahara, R. Suzuki-Migishima, M. Yokoyama, K. Mishima, I. Saito, H. Okano, N. Mizushima, Suppression of basal autophagy in neural cells causes neurodegenerative disease in mice, Nature. 441 (2006) 885–889.

[16] M. Komatsu, S. Waguri, T. Chiba, S. Murata, J. Iwata, I. Tanida, T. Ueno, M. Koike, Y. Uchiyama, E. Kominami, K. Tanaka, Loss of autophagy in the central nervous system causes neurodegeneration in mice, Nature. 441 (2006) 880–884.

[17] N. Mizushima, T. Hara, Intracellular quality control by autophagy: How does autophagy prevent neurodegeneration?, Autophagy. 2 (2006) 302–304.

[18] Y. Kabeya, N. Mizushima, T. Ueno, A. Yamamoto, T. Kirisako, T. Noda, E. Kominami, Y. Ohsumi, T. Yoshimori, LC3, a mammalian homologue of yeast Apg8p, is localized in autophagosome membranes after processing, EMBO J. 19 (2000) 5720–5728.

[19] V. Warrier, M. Vieira, S.E. Mole, Genetic basis and phenotypic correlations of the neuronal ceroid lipofusinoses, Biochim. Biophys. Acta - Mol. Basis Dis. 1832 (2013) 1827–1830.

[20] M. Thelen, M. Dαμμe, M. Schweizer, C. Hagel, A.M.S. Wong, J.D. Cooper, T. Braulke, G. Galliciotti, Disruption of the Autophagy-Lysosome Pathway Is

Involved in Neuropathology of the nclf Mouse Model of Neuronal Ceroid Lipofuscinosis, PLoS One. 7 (2012) e35493.

Figure legends

Figure 1. Specific interactions between TMαBC and CLN6.

HeLa cells were co-transfected with a vector expressing EGFP-tagged CLN6 (CLN6) in combination with a vector encoding myc-tagged wild-type (WTαBC) or ER-anchored (TMαBC) αBC. Whole cell lysates (Input) and the GFP immunoprecipitates (IP: GFP), both derived from the co-transfected cells, were immunoblotted with the indicated antibodies.

Figure 2. CLN6 knockdown attenuated TMαBC's anti-aggregate activity toward the R120G mutant.

(A) HeLa cells were transfected with either siRNA against CLN6 (siCLN6a, siCLN6b) or a scrambled control siRNA (Sc). At 24 h post-transfection, transcript levels of *CLN6* and *Act-b* were examined by RT-PCR.

(B) Protein levels of CLN6 and actin in HeLa cells transfected with the indicated siRNAs were examined at 40 h post-transfection by immunoblotting.

(C) HeLa cells were sequentially transfected with the indicated siRNAs, and with the EGFP-tagged R120G mutant (R120G) plus TMαBC. After 16 h, the cells were imaged with a fluorescence microscope. Scale bars: 20μm

(D) Based on EGFP images in (C), the percentage of cells with aggregates in EGFP-positive cells was calculated. The data is expressed as means ± SEM of seven independent experiments. *$p < 0.05$. At least 800 cells were analyzed for each condition in every assay.

Figure 3. *CLN6 prevented aggregate formation independently of TMαBC.*

(A) Whole cell lysates from HeLa cells co-transfected with the EGFP-tagged R120G mutant (R120G) plus either myc-tagged WTαBC, TMαBC or CLN6 were immunoblotted with antibodies against myc or actin.

(B) The cells were co-transfected as in (A), subjected to microscopic analysis. Shown is the percentage of cells with aggregates in EGFP-positive cells, calculated in the same way as Fig. 2D. The data is expressed as means ± SEM of seven independent experiments. *$p < 0.01$. At least 800 cells were analyzed for each condition in every assay.

(C) Shown is the percentage of cells with aggregates in EGFP-positive cells. Cells were sequentially transfected with the indicated siRNAs and the R120G mutant under the same experimental condition as that in Fig. 2C. The data is expressed as means ± SEM of seven independent experiments. *$p < 0.01$. At least 800 cells were analyzed for each condition in every assay.

(D) HeLa cells were co-transfected with the myc-tagged CLN6 (CLN6) plus either EGFP or the R120G mutant tagged with EGFP (R120G-EGFP). Whole cell lysates (Input) and the myc immunoprecipitates (IP: Myc) were derived from the co-transfected cells, subjected to immunoblotting with the indicated antibodies.

Figure 4. *The autophagy-lysosome system was required for CLN6's anti-aggregate activity.*

(A) The EGFP-tagged R120G mutant and the myc-tagged CLN6 were co-expressed in HeLa cells. At 16 h post-transfection, the cells were treated with either Bafilomycin A1 or MG132, incubated for another 3 h, and then microscopically analyzed for aggregate positivity as in Fig. 2D. The data is expressed as means ± SEM of six independent experiments. *$p < 0.01$. At least 800 cells were analyzed for each condition in every assay.

(B) Whole cell lysates of HeLa cells transfected with either siRNA against ATG5 (siATG5) or a scrambled control siRNA (Sc) were immunoblotted with the indicated antibodies.

(C) Shown is the percentage of cells with aggregates in EGFP-positive cells. Cells were sequentially transfected the indicated siRNAs and the combinations of expression constructs, subjected to microscopic analysis for aggregate positivity as in Fig. 2C. The data is expressed as means ± SEM of seven independent experiments. $^{**}p < 0.01$, $^{*}p < 0.05$. At least 800 cells were analyzed for each condition in every assay.

(D) Whole cell lysates of HeLa cells co-transfected with the indicated combinations of expression constructs were analyzed by immunoblotting with antibodies against LC3-I/II or actin.

Supplementary Figure 1. *Detection of proteins specifically binding to TMαBC.* The myc immunoprecipitates derived from HeLa cells transfected with expression constructs encoding either myc-tagged TMαBC or WTαBC, or with the control empty vector were separated by SDS-PAGE, visualized by silver staining. Protein bands indicated with arrows were excised, subjected to mass spectrometric analysis.

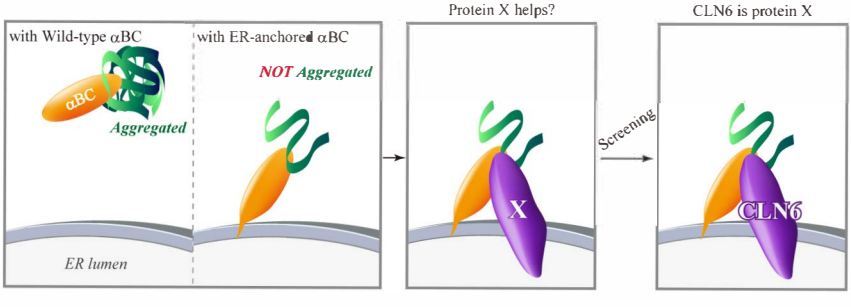

Graphical abstract

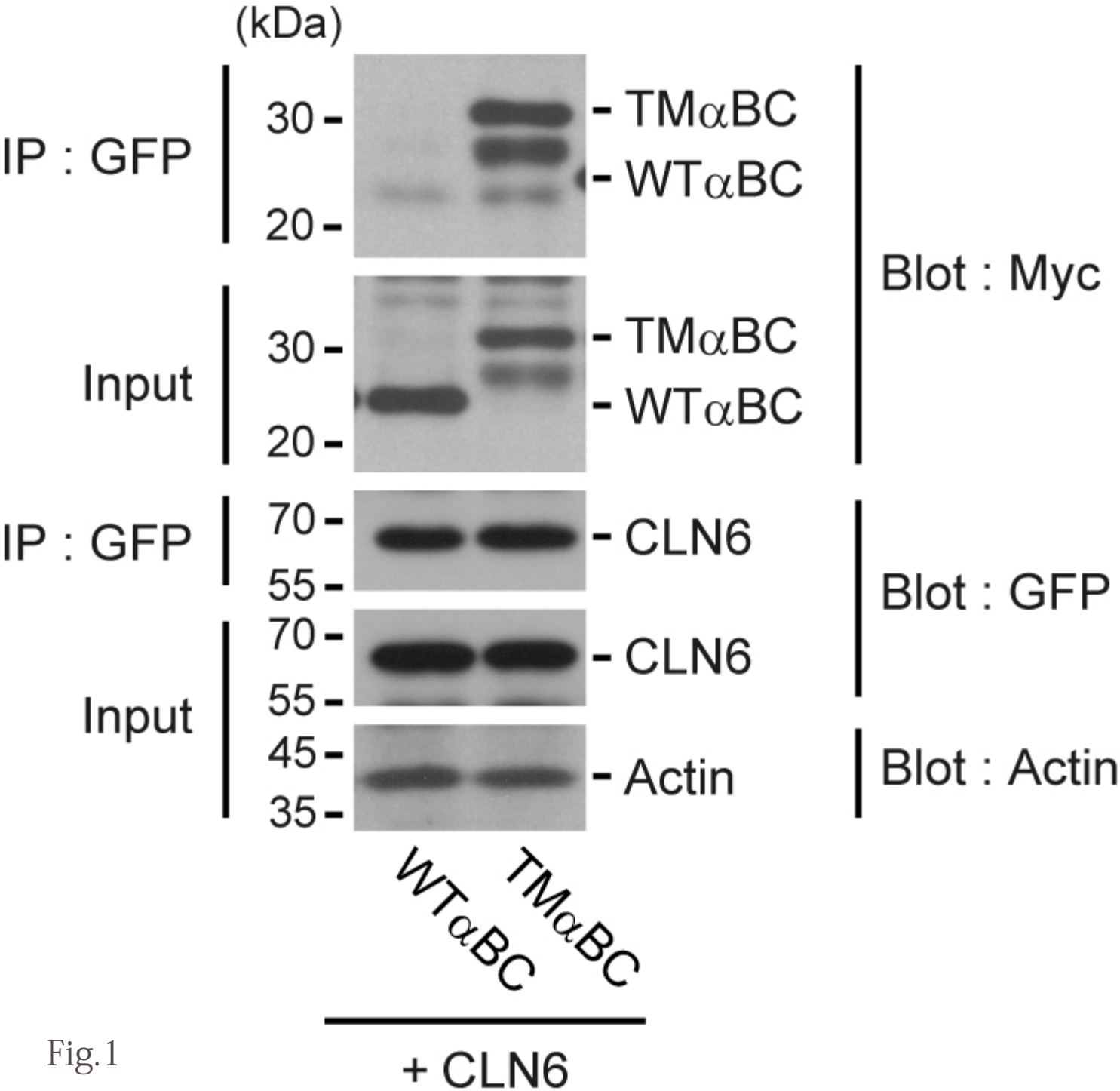
(kDa)
IP : GFP
30
20
TMαBC
WTαBC
Blot : Myc
Input
30
20
TMαBC
WTαBC
IP : GFP
70
55
CLN6
Blot : GFP
Input
70
55
CLN6
45
35
Actin
Blot : Actin
WTαBC
TMαBC
+ CLN6

Fig.1

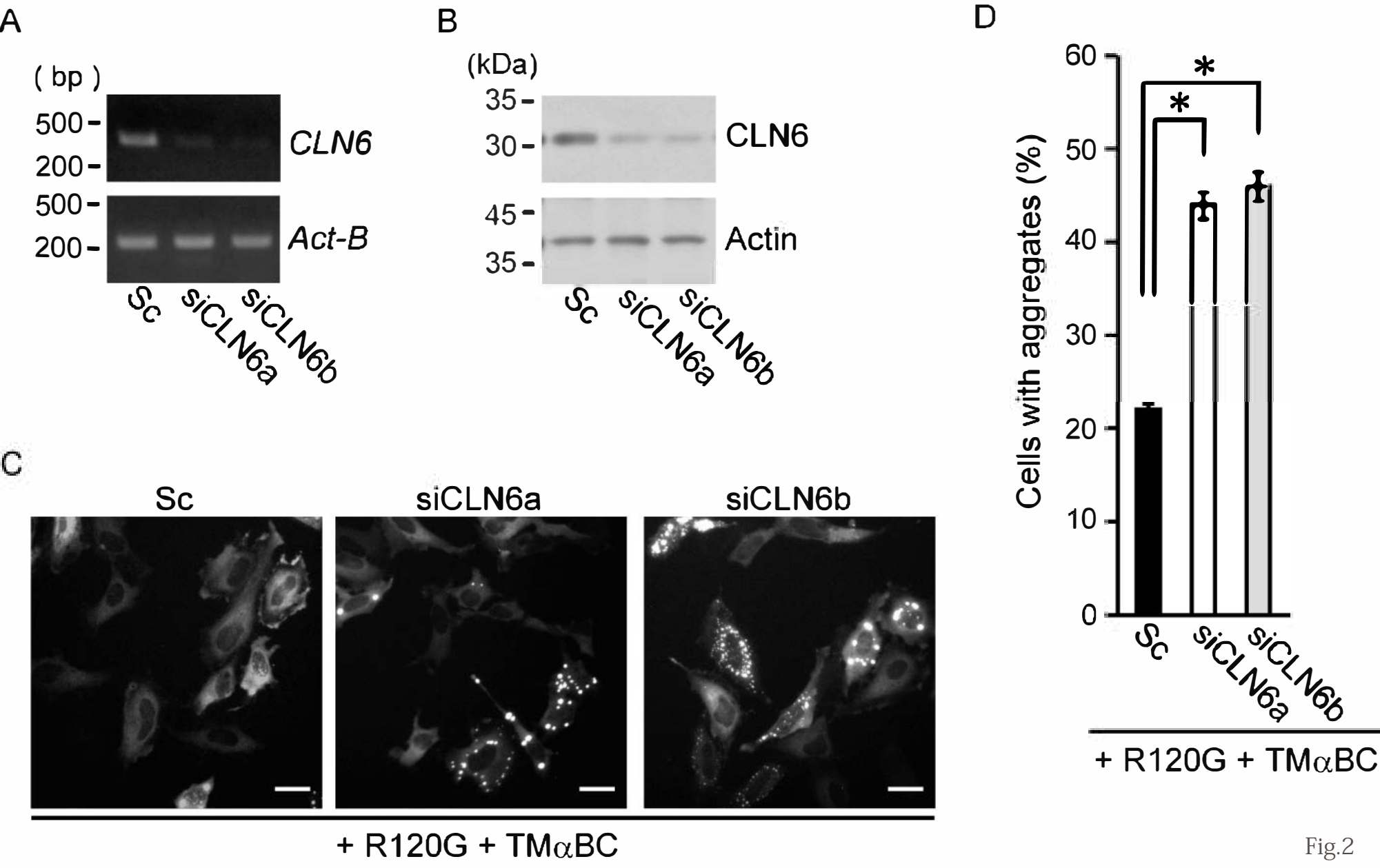
A
(bp)
500
200
CLN6
500
200
Act-B
Sc
siCLN6a
siCLN6b
B
(kDa)
35
30
CLN6
45
35
Actin
Sc
siCLN6a
siCLN6b
C
Sc
siCLN6a
siCLN6b
+ R120G + TMαBC
D
Cells with aggregates (%)
60
50
40
30
20
10
0
*
*
Sc
siCLN6a
siCLN6b
+ R120G + TMαBC

Fig.2

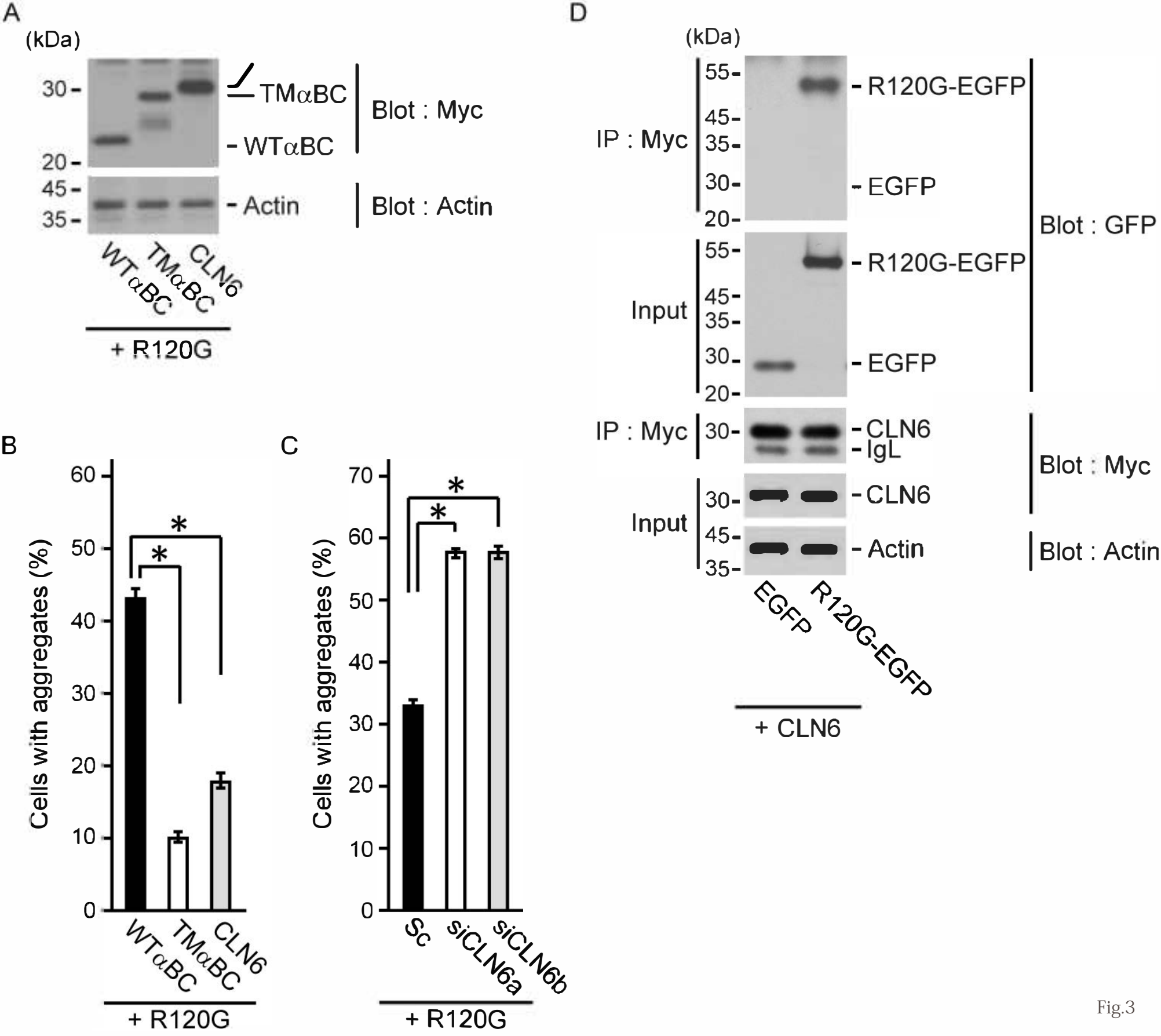
A
(kDa)
30
20
45
35
TMαBC
WTαBC
Actin
Blot : Myc
Blot : Actin
WTαBC
TMαBC
CLN6
+ R120G
B
Cells with aggregates (%)
60
50
40
30
20
10
0
*
*
WTαBC
TMαBC
CLN6
+ R120G
C
Cells with aggregates (%)
70
60
50
40
30
20
10
0
*
*
Sc
siCLN6a
siCLN6b
+ R120G
D
(kDa)
IP : Myc
Input
55
45
35
30
20
R120G-EGFP
EGFP
Blot : GFP
IP : Myc
Input
30
CLN6
IgL
Actin
Blot : Myc
Blot : Actin
EGFP
R120G-EGFP
+ CLN6

Fig.3

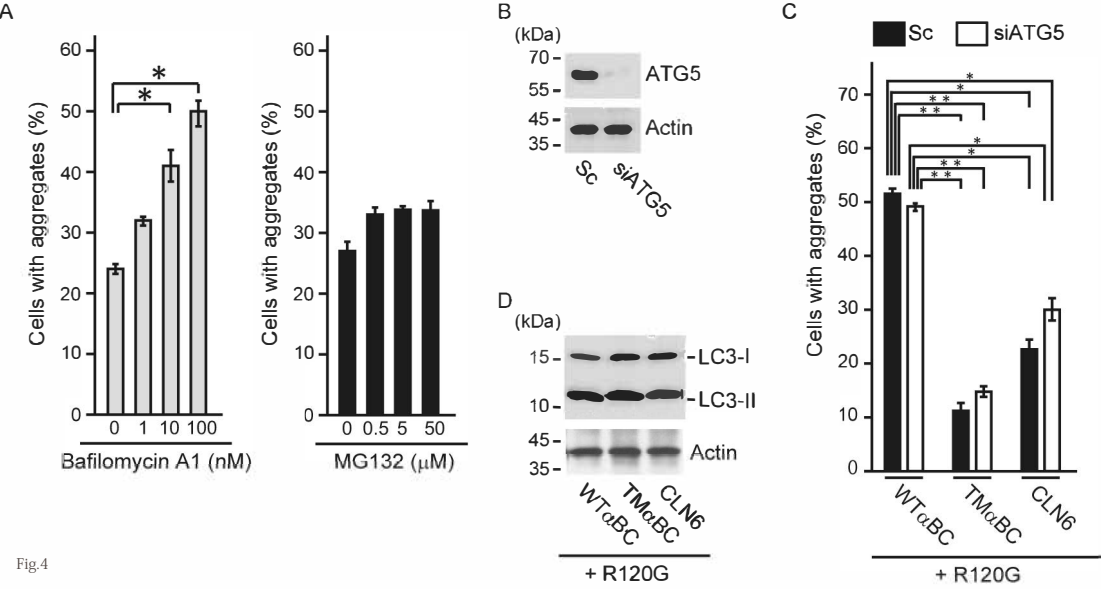
A
Cells with aggregates (%)
60
50
40
30
20
10
0
*
*
0 1 10 100
Bafilomycin A1 (nM)
Cells with aggregates (%)
0 0.5 5 50
MG132 (μM)
B
(kDa)
70
55
45
35
ATG5
Actin
Sc
siATG5
C
Sc
siATG5
Cells with aggregates (%)
WTαBC
TMαBC
CLN6
+ R120G
D
(kDa)
15
10
45
35
LC3-I
LC3-II
Actin
WTαBC
TMαBC
CLN6
+ R120G

Fig.4